

Electronic Supplementary Information for

Directed Assembly of Functionalized Nanoparticles with

Amphiphilic Diblock Copolymers

Yaru Zhou,^a Xiaodong Ma,^a Liangshun Zhang*^a and Jiaping Lin*^a

^aShanghai Key Laboratory of Advanced Polymeric Materials, State Key Laboratory of Bioreactor Engineering, Key Laboratory for Ultrafine Materials of Ministry of Education, School of Materials Science and Engineering, East China University of Science and Technology, Shanghai 200237, China.

*Corresponding Author E-mail: zhangls@ecust.edu.cn (Zhang L.); jlin@ecust.edu.cn (Lin J.)

Contents

Part A: Coarse-Grained Model and Simulation Method

Part B: Probability Distributions of Angle and Distance

Part C: Coordination Number of Nanoparticles

Part D: Effect of Number of Nanoparticles

Part E: Effect of Initial Configuration of Nanoparticles

Part A: Coarse-Grained Model and Simulation Method

We use a coarse-grained model to represent the amphiphilic AB diblock copolymers tethered onto the nanoparticles (NPs), which is illustrated in Figure 1a of the main text. The non-bonded interactions between NP-A, NP-B, A-A and A-B coarse-grained beads are described by the Weeks-Chandler-Andersen (WCA) potential $U_{\text{WCA}}=4\epsilon[(\sigma/r)^{12}-(\sigma/r)^6]+ 4\epsilon[(\sigma/r_{\text{cut}})^{12}-(\sigma/r_{\text{cut}})^6]$ (Figure 1b), where ϵ is the interaction strength and σ the bead diameter. The cutoff distance is set as $r_{\text{cut}}=2^{1/6}\sigma$. The strength for the NP-A, NP-B and A-B interactions is set as $\epsilon=1.0$, while the strength for the A-A interaction is set as $\epsilon=2.0$. The WCA potential is purely repulsive, so the NPs and the A blocks are not solvophobic anymore. The non-bonded interactions between the B-B beads are characterized by the standard Lennard-Jones (LJ) potential $U_{\text{LJ}}=4\epsilon[(\sigma/r)^{12}-(\sigma/r)^6]$, where the interaction strength is set as $\epsilon=2.0$ and $r_{\text{cut}}=2.5\sigma$. These parameter settings imply that only the B beads are solvophobic in the systems. All bonded beads in the polymer chains are connected by a form of harmonic bond potentials $U_b=k_b(r-r_0)^2/2$, where the bond potential constant $k_b=120\epsilon/\sigma^2$ and the bond length $r_0=\sigma$. To control the flexibility of polymer chains, the harmonic angle potential of consecutive beads is introduced by $U_a=k_a(\theta-\theta_0)^2/2$, where $k_a=3\epsilon$ is the angle potential constant and θ_0 is the equilibrium angle with $\theta_0=0.7851$.

We use Brownian dynamics to simulate the systems through the choice of interaction potential as well as drag and thermal noise terms. The periodic boundary conditions are applied in each direction of simulation boxes. The bead motions in the systems obey the equations $m\mathbf{r}''(t)=\mathbf{F}^C+\mathbf{F}^R-\Gamma\mathbf{v}(t)$, where \mathbf{r} and \mathbf{v} are respectively the position and velocity of beads. Γ is the friction coefficient and fixed at $\Gamma=1.0$. \mathbf{F}^C is the total force contributing from

the bonded and non-bonded potentials. The effect of the solvents is implicitly treated by the random force F^R , satisfied the fluctuation-dissipation theorem. The coupling between the friction and random forces acts as an effective thermostat. The integrated time step is fixed at $\Delta t = 0.001\tau$ (τ is the time unit of simulations). All the simulations are performed with HOOMD package on NVIDIA K40 GPU.^{S1, S2}

Sparked by recent experimental works of hierarchical self-assembly,^{S3, S4} we theoretically design the step-wise process to direct the assembly of copolymer-functionalized nanoparticles *via* the coarse-grained simulations. For given parameter settings of such systems, each simulation undergoes two steps: patch formation of single nanoparticles (1st step) and directed assembly of multiple patch-like nanoparticles (2nd step). Meanwhile, each step contains two stages: randomization and equilibrium. Below, we present the detailed procedures for the simulations of copolymer-functionalized nanoparticles. 1st step (patch formation of single nanoparticles): we focus on the system of single nanoparticles tethered by the amphiphilic diblock copolymers, experimentally corresponding to the condition of extremely dilute solution. In the randomization stage, all beads are modeled by the WCA potential for 1×10^6 time steps. Subsequently, the equilibration is simulated for 2×10^7 time steps *via* changing the WCA potentials for the B-B beads to the LJ potentials. 2nd step (directed assembly of multiple patch-like nanoparticles): The patch-like nanoparticles with a specific structure obtained from the 1st step are randomly distributed in the simulation boxes with edge length 100σ , and are randomized for 4×10^7 time steps (note that the patch-like nanoparticles are treated as a rigid body at this stage). In the equilibration stage, the interaction of B-B beads is set as the attractive LJ potential. The systems are equilibrated for

1.5×10^8 time steps to obtain the final configurations.

Part B: Probability Distributions of Angle and Distance

Internal flexibility of patch-like nanoparticles plays a fundamental role in the thermodynamics and kinetics of multiple nanoparticles in the course of directed assembly. Thus, it is important to characterize the arrangement of patches on the isotropic nanoparticles. Here, we calculate the probability distributions of angle between two patches and distance between the centers of patches and nanoparticle, which are depicted in Figure S1. The corresponding definitions of angle and distance are illustrated in inset of Figure S1. In the plot of Figure S1a, all the curves display peaks around the values that reflect the numbers of patches: for two and three patches, the positions of peaks are slightly smaller than π and $2\pi/3$, respectively. For the number of tethered copolymer chains $f=6$, the probability distribution of angle is broad. As the number f of tethered copolymer chains is increased, the distribution becomes narrow, implying that the internal flexibility becomes weak and the corresponding stiffness become strong. In the plot of Figure S1b, we observe a monotonic variation of the average distance and a narrow distribution of distance in response to the number of tethered chains.

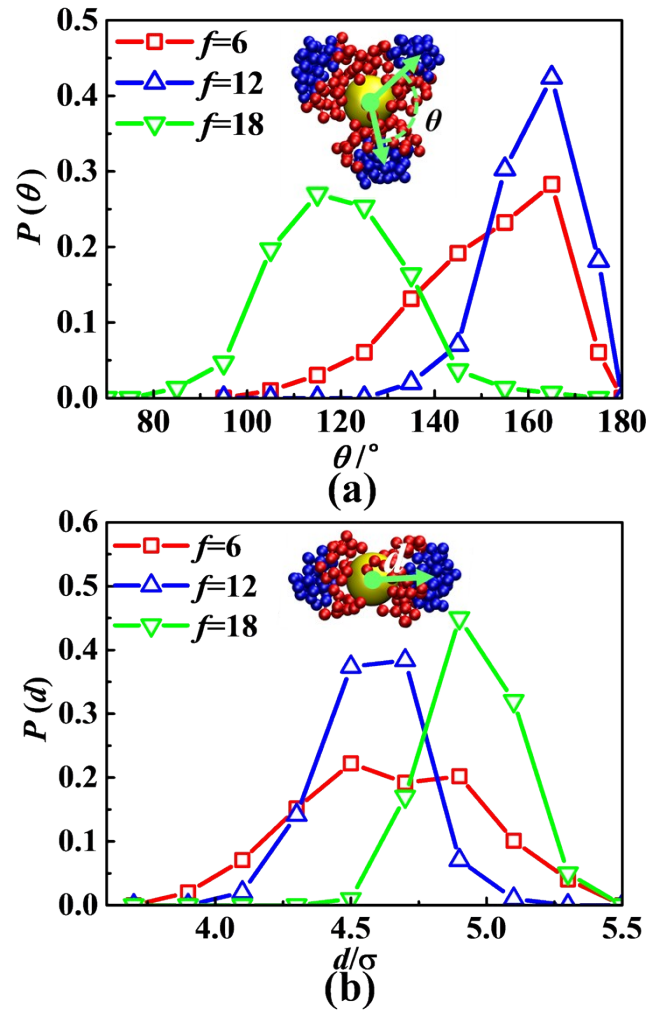


Figure S1. Probability distributions of (a) angles θ between two patches and (b) distance d between the centers of patches and nanoparticle at different numbers of tethered copolymer chains $f=6, 12$ and 18 . Insets of panels (a) and (b) schematically illustrate the definitions of angle θ and distance d . The composition of tethered copolymer chains is fixed at $\alpha=0.5$.

Part C: Coordination Number of Nanoparticles

In order to further identify the assembled superstructures of functionalized nanoparticles, the coordination number of patch-like nanoparticles is calculated for each parameter setting and its distribution is shown in Figure S2a. For the copolymer-functionalized nanoparticles with $f=6$ and 9, the formed Janus-type nanostructures are directed to assemble into the micelle-like superstructures, where the coordination numbers are mainly distributed between 2 and 4. In the cases of $f=12$ and 15, most of the patch-like nanoparticles within the superstructures have the coordination number of 2. Figure S2b shows the average coordination number of patch-like nanoparticles within the superstructures in terms of the number of tethered copolymer chains. It is demonstrated that the coordination numbers of nanoparticles within the micelle-like superstructures are close to 3, whereas those within the chain-like superstructures approach 2.

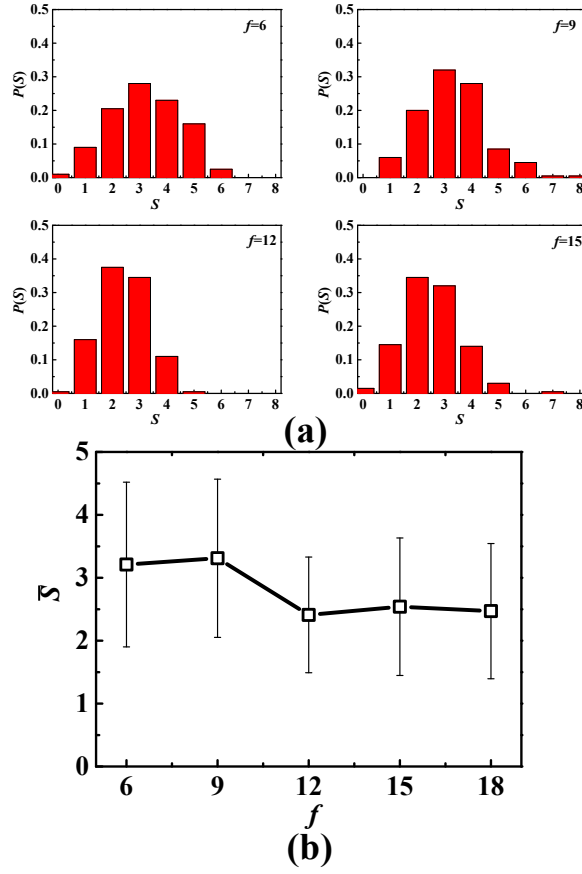


Figure S2. (a) Distribution $P(S)$ of coordination number of functionalized nanoparticles under various numbers of tethered copolymer chains $f=6, 9, 12$ and 15 . (b) Average coordination number \bar{S} of nanoparticles within the superstructures in terms of the number f of tethered copolymer chains. The composition of tethered copolymer chains is set as $\alpha=0.25$. The error bars stand for the standard deviations (SD). The average values and the standard

deviations are defined as $\bar{S} = \sum_j P(S_j) S_j$ and $SD = \left(\sum_j P(S_j) (S_j - \bar{S})^2 \right)^{1/2}$, respectively.

Part D: Effect of Number of Nanoparticles

In the range of number of nanoparticles between 20 to 50, the copolymer-functionalized nanoparticles are directed to assemble into the chain-like superstructures under the parameter settings $f=9$ and $\alpha=0.50$ (Figure S3). It should be mentioned that the branched chains of nanoparticles are also observed as the number of nanoparticles is increased.

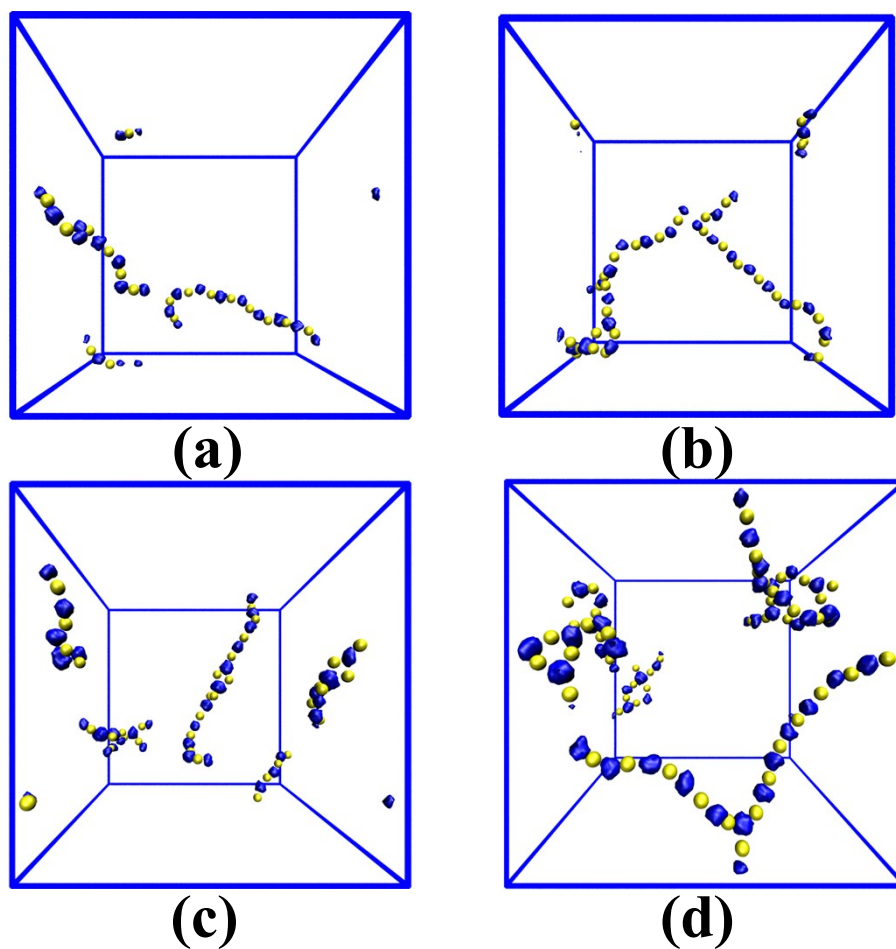


Figure S3. Hierarchically assembled superstructures of copolymer-functionalized nanoparticles under various numbers N of patch-like nanoparticles in the simulation boxes. (a) $N=20$, (b) $N=30$, (c) $N=40$ and (d) $N=50$. Note that the edge length of simulation boxes is fixed at 100σ . The number and composition of tethered copolymer chains are set as $f=9$ and $\alpha=0.50$, respectively.

Part E: Effect of Initial Configuration of Nanoparticles

In the main text, the patch-like nanoparticles serve as the pre-assembled entities for the next-level hierarchical assembly. This kind of directed assembly leads to a stepwise reduction of conformational freedom degrees and avoids undesirable kinetic obstacles during the structural build-up. As demonstrated in Figures 4b and 6b in the main text, the patch-like nanoparticles assemble into the linear chain-like superstructures with occasionally defects. As a comparison, we simulate the formation of superstructures, starting from an initially random configuration of nanoparticles tethered by the stretchable diblock copolymers. We switch the solvents from good to poor for the outer B blocks at the beginning of simulations. The snapshots for the formation of superstructures are displayed in Figure S4a. In the early stage, the diblock copolymers tethered onto the spherical surfaces start to form small patches, which are similar with the case shown in Figure 2 of main text. Meantime, mutual attachments of such soft nanoparticles with small patches take place, leading to various valences of patch-like nanoparticles in the simulation boxes. The subsequent coalescence of oligomers with the trivalent nanoparticles results in production of highly branched arrangement of nanoparticles, which is depicted in Figure S4b. In comparison with the assembled superstructures from various initial configurations of nanoparticles (Figure 6b and Figure S4b), one can identify that the well-defined superstructures are achieved *via* introduction of pre-assembly building entities.

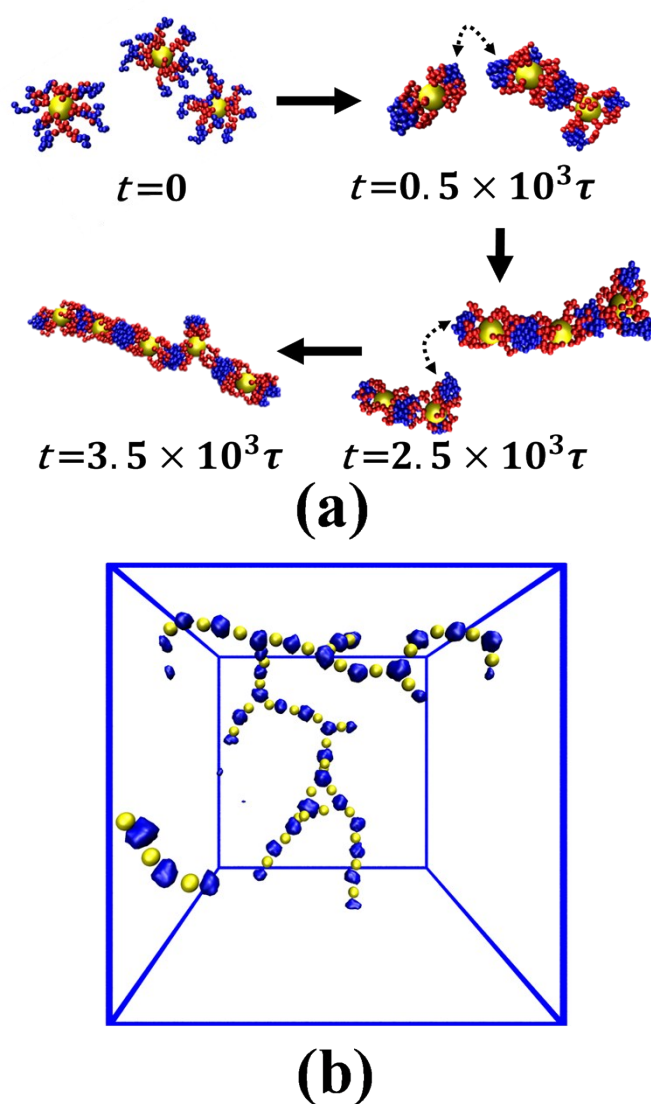


Figure S4. (a) Formation of chain-like superstructures from initial configuration of nanoparticles tethered by stretchable diblock copolymers. The straight arrows indicate the time sequence. The bent dashed arrows point from the patch to the site where it is going to attach. (b) Final configuration of assembled superstructures of copolymer-functionalized nanoparticles. The number and composition of tethered copolymer chains are set as $f=12$ and $\alpha=0.5$, respectively.

References

- S1 J. A. Anderson, C. D. Lorenz and A. Travasset. *J. Comp. Phys.*, 2008, **227**, 5342-5359.
- S2 J. Glaser, T. D. Nguyen, J. A. Anderson, P. Lui, F. Spiga, J. A. Millan, D. C. Morse and S. C. Glotzer, *Comput. Phys. Commun.*, 2015, **192**, 97-107.
- S3 A. H. Gröschel, F. H. Schacher, H. Schmalz, O. V. Borisov, E. B. Zhulina, A. Walther and A. H. E. Müller, *Nature Commun.*, 2012, **3**, 710.
- S4 A. H. Gröschel, A. Walther, T. I. Löbbling, F. H. Schacher, H. Schmalz and A. H. E. Müller, *Nature*, 2013, **503**, 247-251.